Hindawi
Wireless Communications and Mobile Computing
Volume 2022, Article ID 9148756, 20 pages
https://doi.org/10.1155/2022/9148756

Research Article

Underwater Acoustic Micromodem for Underwater Internet of Things

Hongbin Chen, Yi Zhu, Wenwen Zhang, Kefei Wu, and Fei Yuan

Key Laboratory of Underwater Acoustic Communication and Marine Information Technology, Xiamen University, Xiamen 361005, China

Correspondence should be addressed to Fei Yuan; yuanfei@xmu.edu.cn

Received 23 May 2022; Accepted 11 August 2022; Published 13 September 2022

Academic Editor: Suhua Tang

Underwater acoustic communication (UAC) networks are becoming a hot spot for research due to the growing demand for ocean development. Previous acoustic modems were mainly designed for the field of ocean engineering construction and scientific investigation, and consequently, with the characteristics of large size and high-power consumption, a low-cost, low-power consuming micromodem is proposed in this paper to satisfy the requirements of underwater Internet of Things (IoT). The STM32F767 processor is embedded in the micromodem as the core for fast digital signal processing. Furthermore, a convolutional code–block interleaving–frequency hopping–MFSK underwater communication scheme is also discussed to ensure the communication quality. Experimental results are shown to demonstrate our modem can realize the reliable UAC transmission of 200~300 bit/s at the distance of 500 m.

1. Introduction

With the increasing degree of exploration, exploitation, and utilization of the ocean, there is a huge demand for communication technology under the marine environment in both the offshore military and civilian fields [1, 2], such as the construction of underwater sensor networks, underwater operations of divers, and underwater unmanned vehicles. Radio frequency (RF) communication commonly used in the terrestrial communication system has very high propagation loss in seawater. Optical communication has strict requirements on device and is easily affected by the environment around the ocean. Underwater acoustic communication (UAC) is the most widely used communication technology in seawater, characterized by long communication distance, low communication rate, and large time delay. However, there are still a series of difficulties and challenges for UAC, such as more serious multipath, time-varying, and the Doppler shift effects. Therefore, it is a great challenge to design a high-performance underwater communication modem that can adapt to the changes of environment.

In recent years, with the development and diversification of UAC technology, many companies have launched their commercial underwater acoustic modems, such as Tritech [3], Sonardyne [4], Teledyne Marine [5], LinkQuest [6], DSPComm [7], and EvoLogics [8]. Their products have their own advantages in terms of communication distance and rate. However, they share the common characteristics of relatively large size and high price, which are not suitable for underwater Internet of Things (IoT) applications that require large-scale deployment of nodes.

In view of the above disadvantages, to reduce the power consumption of UAC modems and improve the cost performance, academic researchers also made a lot of attempts. Bin Abbas et al. [9] designed a software-defined radio-(SDR-) based underwater acoustic modem with a rate of 100 bit/s and reached 70% data reception at 25 m in a lake test. The "Seatrac" acoustic modem based on spread spectrum communication was proposed by Neasham et al. [10], connecting divers and subsea robotics with the communication rate of 100 bit/s around 1.5 km and bit error rate (BER) below 10^{-2}. Li et al. [11] presented a low power

Table 1: Parameters of proposed modem and state-of-the-art methods.

Underwater acoustic modem	Processing	Price ($)	Dimension (mm)	Modulation	Frequency band (kHz)
Proposed	MCU	ca. 500	$\Phi 64 \times 40$	FH–MFSK	35-45
Commercial devices					
Tritech Micron Modem	n.a.	ca. 19000	$\Phi 56 \times 79$	n.a.	20-28
Sonardyne modem 6 submini	n.a.	ca. 15000	$\Phi 75 \times 420$	n.a.	21-31.5
Teledyne benthos ATM-964	n.a.	ca. 20000	$\Phi 127 \times 741$	PSK	9-27
LinkQuest UWM2000	n.a.	ca. 24000	$\Phi 126 \times 250$	n.a.	26.77-44.62
DSPComm Aquacomm Gen2	DSP	ca. 15000	$100 \times 70 \times 20$	DSSS/OFDM	16-30
EvoLogics S2CT 42/65	FPGA	ca. 25000	$\Phi 63 \times 170$	n.a.	42-65
Devices developed by research groups					
[9]	PC	n.a.	n.a.	FSK	14-17.5
[10]	MCU	n.a.	$\Phi 55 \times 160$	Chirp-BOK	24-32
[11]	MCU	n.a.	n.a.	n.a.	n.a.
[12]	Arduino	n.a.	n.a.	s	n.a.
[13]	MCU	n.a.	$\Phi 70 \times 40$ (board)	n.a.	n.a.
[14]	MCU	n.a.	n.a.	FSK	20-40
[15]	MCU	ca. 600	$50 \times 50 \times 25$	FSK, OFDM	25-87.5
[16]	MCU	n.a.	120×45	MC–MFSK	20-30

Table 2: Continuation of Table 1.

Underwater acoustic modem	Data rate	BER	*Tx* power (W)	*Rx* power (mW)	Idle (mW)	Range (m)
Proposed	200-300 bps	10^{-3}	6	600	2.4	>500
Commercial devices						
Tritech Micron Modem	40 bps	n.a.	7.92	720	n.a.	500
Sonardyne modem 6 submini	200-9000 bps	n.a.	n.a.	n.a.	n.a.	1000-1500
Teledyne benthos ATM-964	80-15360 bps	n.a.	20	700	12	2000-6000
LinkQuest UWM2000	17800 bps	10^{-9}	8	800	8	1500
DSPComm Aquacomm Gen2	100-1000 bps	10^{-6}	12/30	n.a.	6-60	8000
EvoLogics S2CT 42/65	Up to 31200 bps	10^{-10}	25	0.8	n.a.	1000
Devices developed by research groups						
[9]	20-600 bps	0-30%	n.a.	n.a.	n.a.	25
[10]	100 bps	10^{-2}	n.a.	n.a.	n.a.	1500
[11]	n.a.	n.a.	0.816	n.a.	0.43	n.a.
[12]	30 bps	n.a.	n.a.	n.a.	n.a.	n.a.
[13]	200-500 bps	10^{-2}	8	n.a.	n.a.	500
[14]	150 bps	n.a.	8	300	8	140
[15]	260-4700	0-30%	5	300	1	150
[16]	125-1007 bps	10^{-2}	n.a.	n.a.	n.a.	2500-8000

consumption modem, which has a minimum transmit/receive power of 816 mW. A low-cost modem with communication structure was introduced by Misra et al. [12] for underwater monitoring. The system can detect events of interest in the water and send information to the base station. For shallow water communication, it can reach the data rate of 30 bit/s. Lee et al. [13] use STM32F103 as the core processor to realize UAC at the speed of 5 kbit/s within a distance of 500 m. A low-power, low-cost underwater sensor node called Proteus II was described in [14], and its acoustic modem uses FSK modulation and is able to communicate 150 bit/s at a range of 140 m in lake experiment. The acoustic modem called ahoi developed by Renner et al. [15] keeps the cost within $600 and can achieve

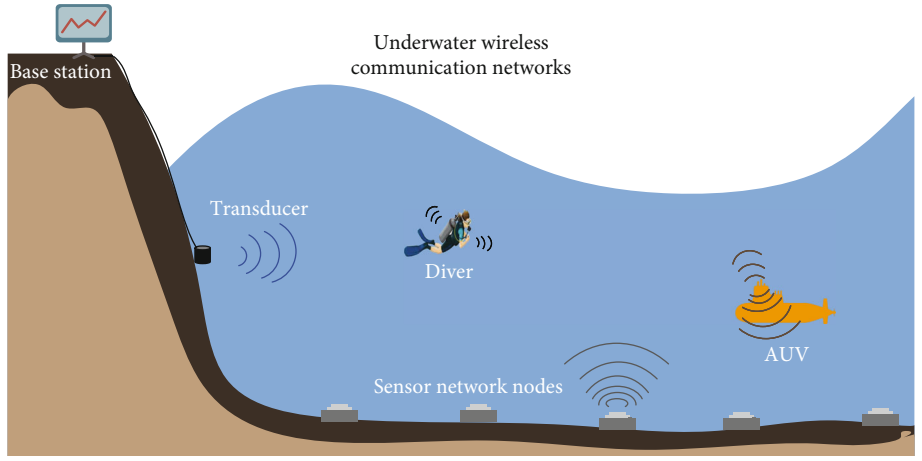

Figure 1: Application scenarios of acoustic micromodem.

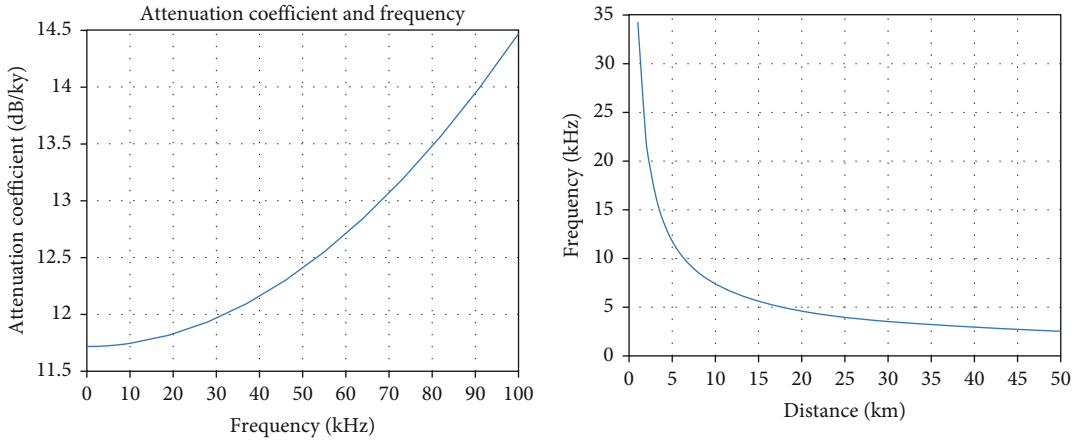

Figure 2: (a) Relationship between the absorption coefficient of seawater and frequency. (b) Relationship between optimal communication distance and frequency.

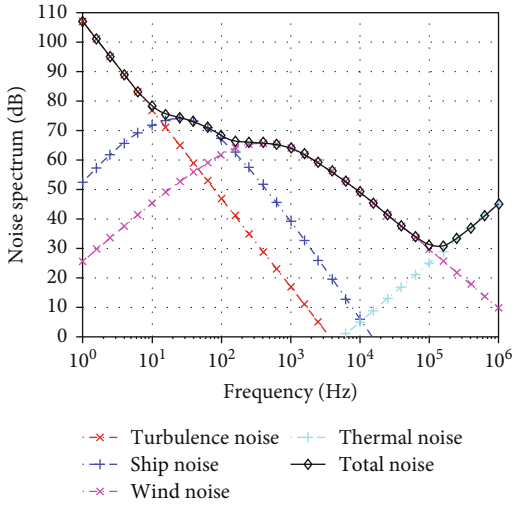

Figure 3: Spectrum levels of environmental noises.

communication over a distance of 150 meters. Su et al. [16] took the STM32H743 processor as the core to implement different communication algorithms on one platform. Parameters of our proposed modem and state-of-the-art methods are summarized in Tables 1 and 2.

In this paper, a low-cost acoustic micromodem is designed and implemented according to the current needs of underwater communication networks. The system is based on the criteria of low cost, low power consumption, light weight, and compactness. It can accomplish reliable communications and meet the needs of low-rate underwater communication applications which are sensitive to cost, size, and battery life. Considering that voice is the most simple and efficient way for information interaction, we also extend a voice module on the modem to implement voice communication for specific commands and enhance its generalizability.

The remaining sections of this paper are organized as follows: Section 2 introduces the application scenarios

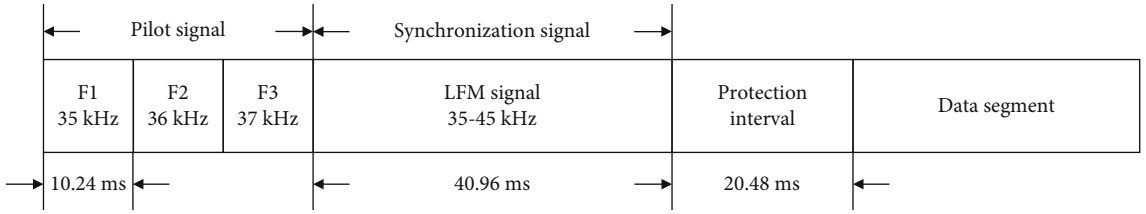

Figure 4: Physical layer frame format.

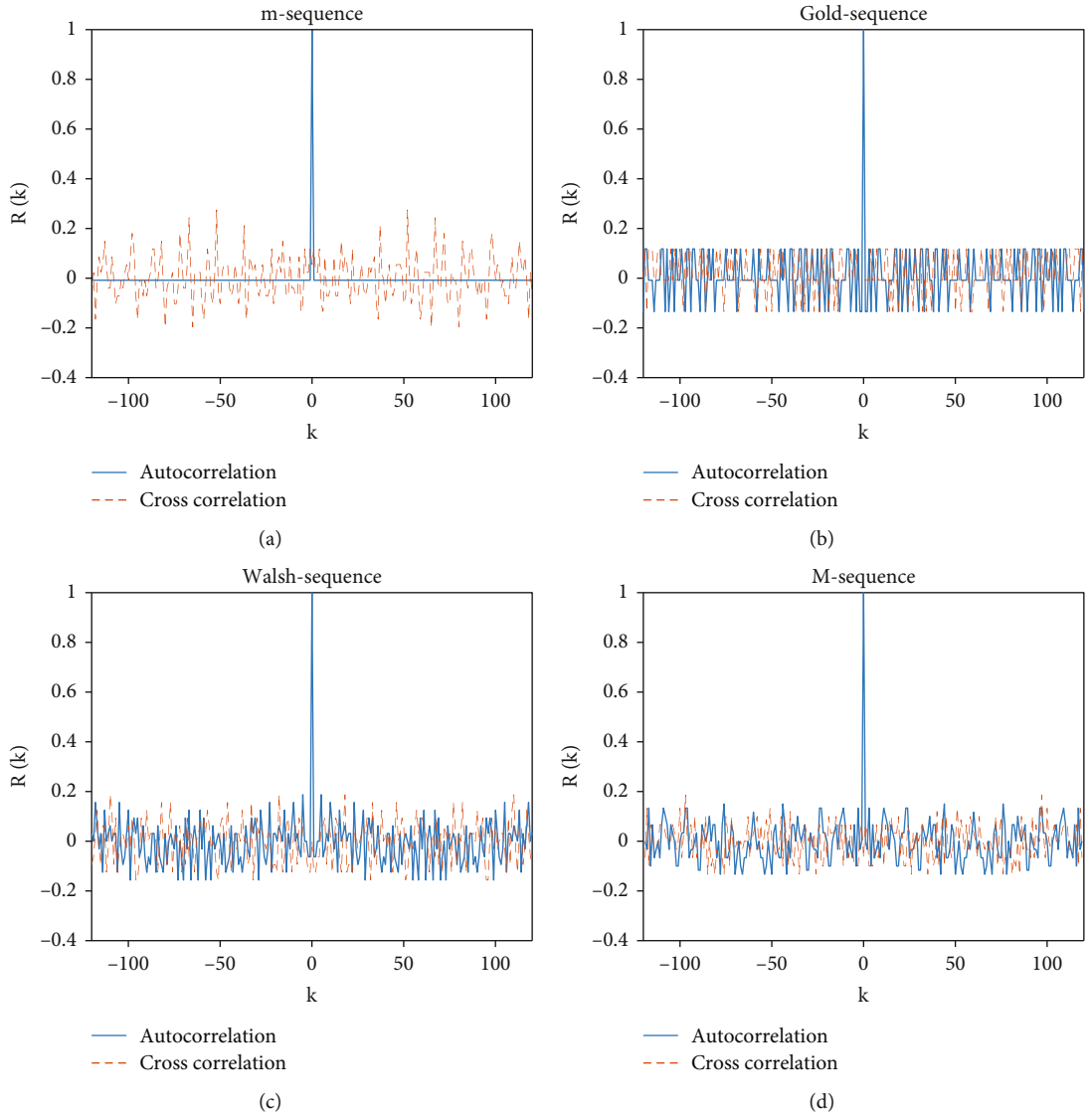

Figure 5: Correlation properties of pseudorandom sequences.

and system overview. Section 3 describes the UAC algorithm scheme, including the design of the frame format. Section 4 introduces the hardware design of our proposed modem. Several tests are carried out in Section 5 to verify the performance of our modem, and the last section concludes with the relevant summary.

2. Application Scenarios and System Description

As shown in Figure 1, our acoustic modem can be used in a variety of underwater communication scenarios within a certain distance and transmission rate. One of the scenarios

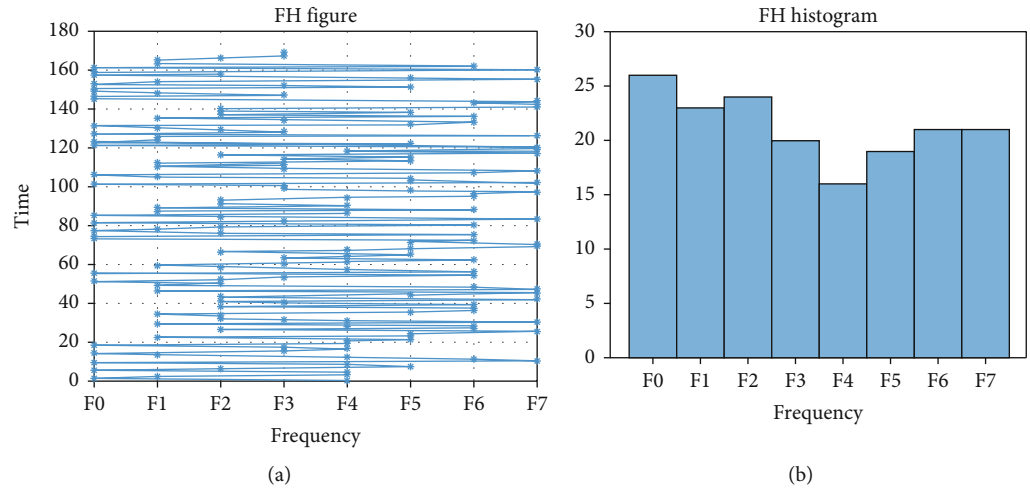

Figure 6: (a) FH figure. (b) FH histogram.

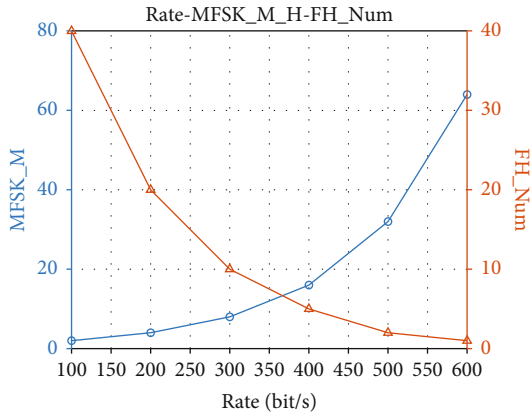

Figure 7: Transmission rate versus M (modulation order) and hopping band.

is underwater wireless sensor network, and our modems are suitable for mass deployment on the bottom of water to connect with buoy nodes. Based on routing protocol, messages can be delivered through multiple modems to maintain a stable, low-rate information exchange between communication nodes and base station and realize the functions of long-distance control, underwater cooperative detection, and data acquisition. Another scenario is autonomous underwater vehicle (AUV). AUV is a kind of unmanned vehicle that can complete tasks under the assistance of base station and surface ships. After AUVs are launched, they can realize complex operations including marine terrain survey and underwater reconnaissance with our modems. The third application scenario is the communication problem of divers. Through our acoustic modem, the surface platform can obtain the status of divers in real time, such as position, vital signs, and other information. Divers can also communicate directly with the platform or other divers at any time. In addition, we also have speech recognition and synthesis module extended on the communication modem to achieve voice communication for some special commands, such as environmental abnormalities and danger warnings. On the other hand, it also ensures that the monitoring platform can notice special situations as soon as possible.

In response to the above scenario requirements, the design objectives of our modem are summarized as follows: (a) the communication distance is within 1 km; (b) low communication rate can be accepted, but high reliability should be kept; and (c) the ability to achieve large-scale deployment applications. Our system parameters of the acoustic modem are designed according to these targets.

2.1. Communication Band. The choice of frequency band of UAC system affects the propagation distance and the size of transducer module. Based on the purpose of developing a miniaturized modem and considering the communication distance about 1 km, the calculations of communication band are as follows.

The near-field transmission loss of acoustic waves becomes

$$TL = 20logr + \alpha r + 60 - k_l, \tag{1}$$

where α is seawater absorption coefficient, r is communication distance, and k_l is abnormal attenuation.

Acoustic wave attenuation includes absorption, scattering, and channel damage. When sound frequency is above 1 kHz, the main factor causing attenuation is the absorption by seawater. The absorption coefficient can be obtained from Thorpe's formula

$$\alpha = \frac{0.1f^2}{1+f^2} + \frac{40f^2}{4100+f^2} + 2.75 \times 10^{-4} f^2, \tag{2}$$

and the frequency is in kHz.

Figure 2(a) illustrates the relationship between the absorption coefficient of seawater and frequency. The higher the frequency, the larger the absorption coefficient. Therefore, the frequency used in medium distance communication is generally not more than 50 kHz in practical applications.

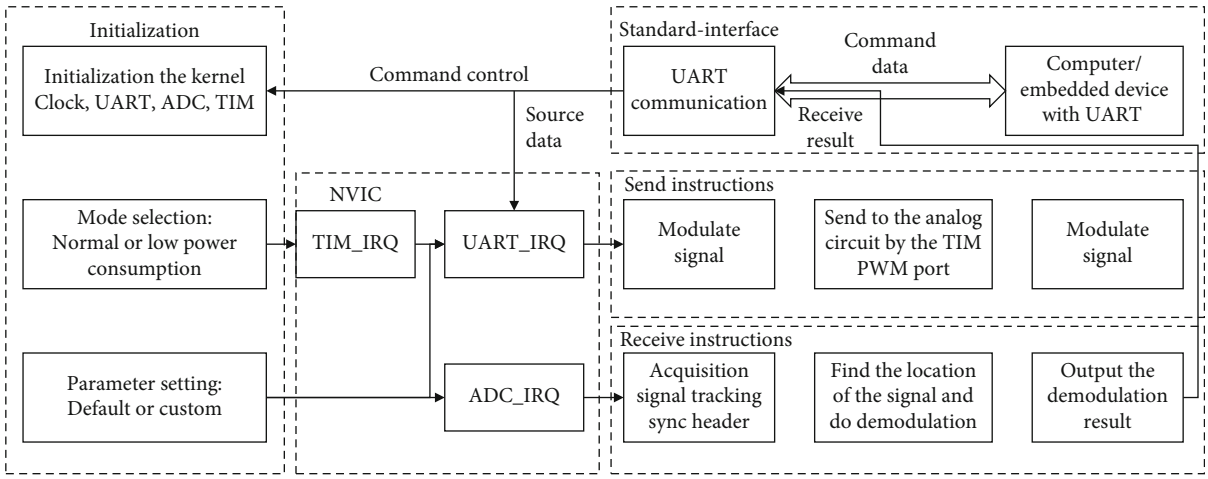

Figure 8: Software flowchart.

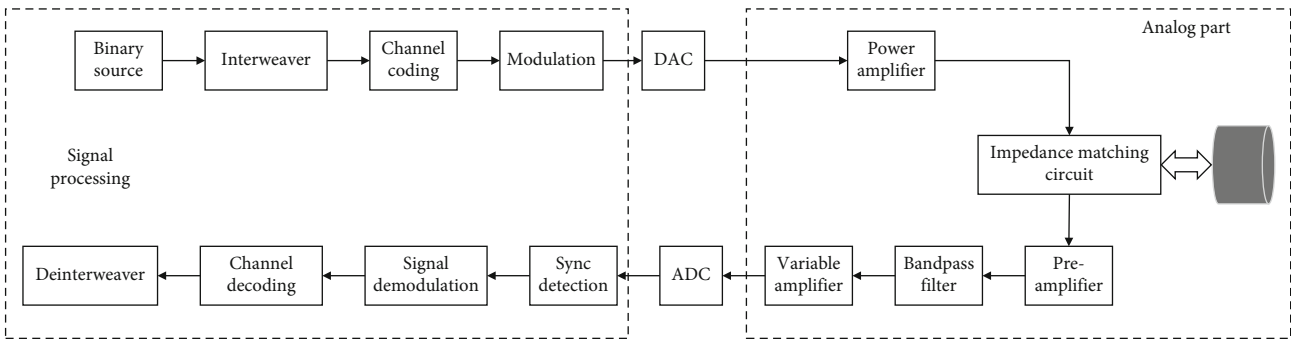

Figure 9: Hardware flowchart.

Figure 2(b) shows the relationship between optimal communication distance and frequency, according to Equation (2). The signal-to-noise ratio (SNR) of the received signal decreases as the frequency increases, resulting in a shorter transmission distance. It is usually considered that the communication distance is in inverse proportion to the square of the sound frequency. It can be seen from the figure that the short-distance UAC frequency can reach 30~50 kHz.

The main application distance of proposed acoustic modem is around 1 km, so the optimal frequency band is above 35 kHz. In general, there is an inverse association between the volume of the underwater acoustic transducer and the frequency of the transmitted signal. Taking these factors into account, the communication band of our acoustic modem is selected from 35 to 45 kHz. Since the center frequency of the system is 40 kHz, we can obtain the seawater absorption rate α is 11.77 dB/km. Assuming the near-field abnormal attenuation k_l is 10 dB, we can get the propagation loss TL as 63.66 dB.

2.2. Emitted Sound Source Level. When underwater acoustic transducer directivity coefficient is zero, the passive sonar equation becomes [17]:

$$DT = SL - TL - NL, \tag{3}$$

where DT represents the detection threshold, SL means transmitting sound level, NL is the ambient noise including marine environmental noise and ship noise, and TL is propagation loss.

It can be seen from Equation (3) that DT is mainly determined by the transmitting sound source level, propagation loss, and environmental noise. The estimation of SL is an important guideline for the design of amplifier. The requirement of SL in our project is given below:

The sound source level is defined as the sound intensity level at a distance of 1 m from the sonar transmitter on the sound axis. Under the condition of free traveling waves, the sound intensity level is equal to the sound pressure level, and the sound source level L_α can be expressed as

$$L_\alpha = L_p + 20 \log_{10} d, \tag{4}$$

where L_p is the measured sound pressure level in dB at a certain point in the far-field diffused by spherical waves in the axial direction of the sound source center and d represents the distance from the measuring point to the center of the sound source in meter.

Underwater sound pressure level mostly adopts the indirect measurement method; it is determined by the open-circuit voltage value and the sensitivity of the hydrophone:

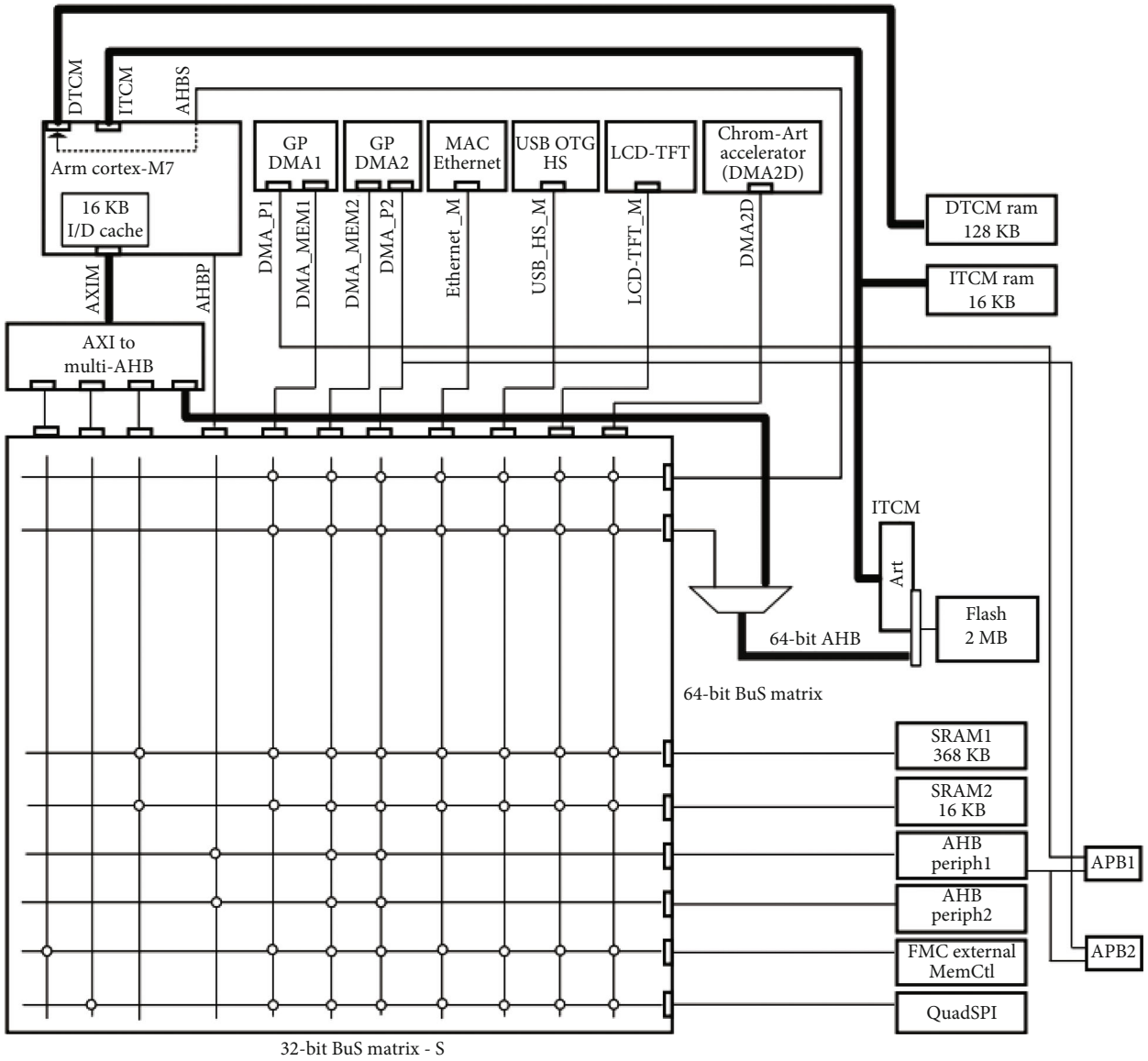

Figure 10: STM32F767 system architecture.

$$P = U_{OC}/M, \tag{5}$$

where U_{OC} indicates the open-circuit voltage of the hydrophone in V and M is the sensitivity value of the hydrophone in V/Pa.

According to Equation (3), when the emitted sound source level is constant, marine environmental noise is another important factor affecting communication and detection except propagation loss. The total noise synthesized by various environmental noises is given by

$$NL_{total} = 10 \log \left(10^{NL_{wind}/10} + 10^{NL_{turbulence}/10} + 10^{NL_{ship}/10} + 10^{NL_{thermal}/10}\right). \tag{6}$$

Figure 3 shows the spectrum levels of environmental noises in the underwater acoustic communication channel under the condition of level 3 ocean conditions and medium shipping density.

In the communication band, the ambient noise spectrum level NL is 44 dB, combined with the theoretical value of TL calculated above; assuming the detection threshold DT is 18 dB, we can get that SL is 125.66 dB from Equation (3). In order to ensure the communication performance of the acoustic modem in practice, the sound source level is generally designed higher than the theoretical value, so our emitted sound source level is above 130 dB.

3. Underwater Acoustic Communication Scheme

For reliable data transmission in underwater communication systems, the frame format of the physical layer is designed as depicted in Figure 4. At the beginning of each frame, three single-frequency signals are inserted to obtain

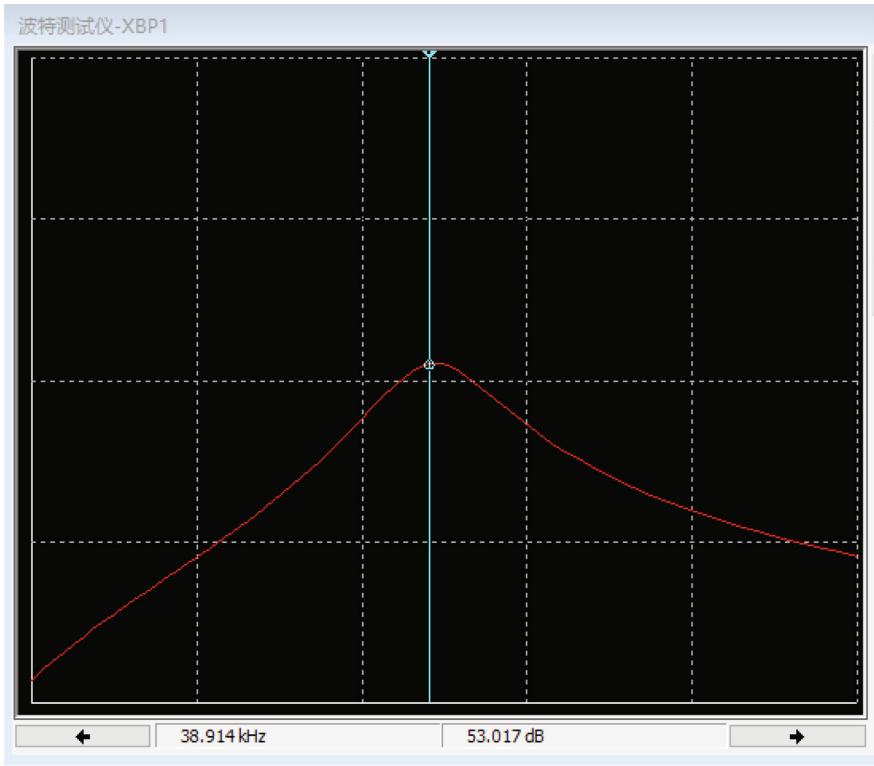

Figure 11: Amplitude-frequency characteristic of designed band-pass filter.

coarse synchronization at the receiver. The following is a linear frequency modulation (LFM) signal, which is used to achieve accurate time synchronization. A blank signal of 20.48 ms is also left between the synchronization signal and user data as a protection interval.

3.1. Synchronization

3.1.1. Coarse Synchronization. In this paper, the single-frequency signals are used as wake-up signal and coarse synchronization signal. The function of coarse synchronization is to make the receiving system start demodulation of fine time synchronization only when the time is closer to the signal, which can effectively reduce the amount of operation and improve the accuracy of synchronization.

The coarse synchronization is calculated by spectrum analysis. A certain time window with a fixed width is set and moved along the time axis of signal. The signal segment observed in the window is transformed to the frequency domain by fast Fourier transform (FFT). If the preset frequency is captured, the time window will be slid left and right to compare the magnitude of frequency energies. The largest energy is considered the time point for this detection and passed to the next detection. Coarse synchronization will be successfully performed if more than two frequencies of F1, F2, and F3 are detected.

3.1.2. Fine Synchronization. The fine synchronization stage takes advantage of the excellent autocorrelation property of LFM signal and uses matched filtering at receiver to achieve accurate detection of the LFM signal. When the LFM signal and the matched signal are consistent in time, the output of the filter is given by

$$g(t) = \sqrt{BT}\cos(2\pi f_0 t)\frac{\sin[\pi Bt(1-(|t|/T))]}{\pi Bt} - T/2 \le t \le T/2. \quad (7)$$

The matched output exhibits a sharp peak at the zero moment, and all the energy of the signal is concentrated in a very short period of time. When there is a time delay in LFM signal, the time point of the maximum value will be offset, and the amplitude will also change. Through the change of peak time, we can calculate the time delay of LFM signal, so as to obtain the precise synchronization position of received signal.

3.2. FH–MFSK Modulation Scheme. A large part of interference in underwater communication comes from multipath signals, which belong to narrowband interference. Frequency hopping (FH) is a kind of spread spectrum communication; it can decrease the intersymbol interference by controlling the carrier frequency hopping through pseudorandom codes. In this paper, we use the frequency hopping–multiple frequency shift keying (FH–MFSK) system for signal modulation. The data to be transmitted is preprocessed by system, and then each carrier is MFSK modulated. Subsequently, the carrier frequency selected by pseudorandom sequence is mixed with the MFSK modulated signal. Finally, the signal is converted into acoustic signal by transducer and transmitted to the underwater acoustic channel. The dehopping system will analyze the received signal for frequency, after mixing it with the same

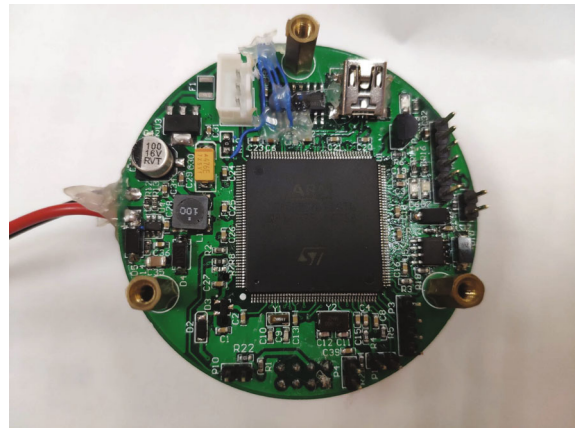

(a)

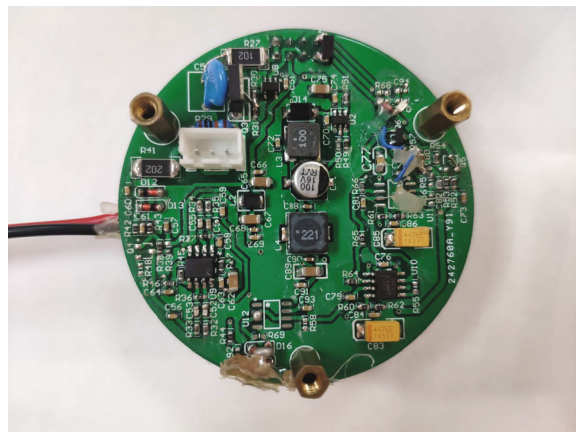

(b)

Figure 12: Experimental prototype of our micromodem. (a) Digital board. (b) Analog board.

Figure 13: The customized sheet ceramic transducer.

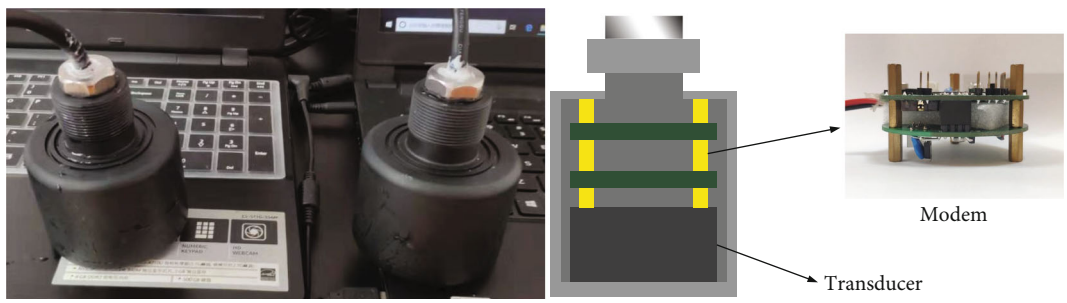

Figure 14: All-in-one package.

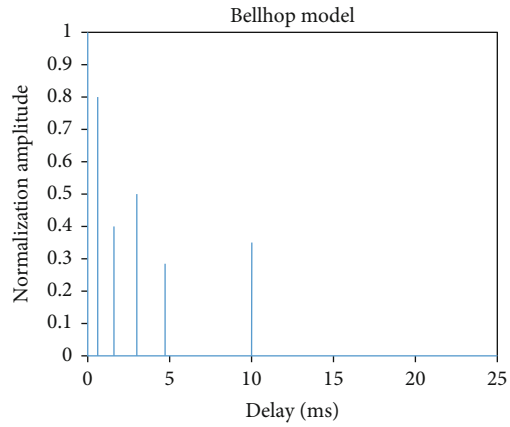

Figure 15: Bellhop multipath model.

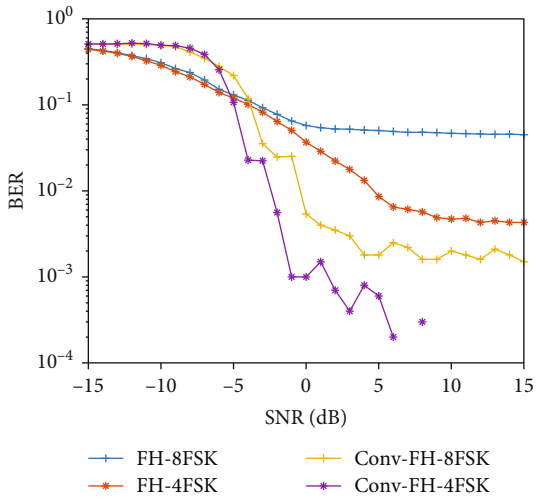

Figure 16: Simulation BER results under multipath channel with 10000 bits.

frequency sequence as transmitter; FSK demodulation is performed, and user data will be restored.

Here are some typical pseudorandom sequences.

The m-sequence is the most basic and commonly used PN sequence. It is generated by the n-level linear shift register, and the length of the sequence is $2^n - 1$. The longer the m-sequence is, the stronger the randomness is, and the closer to the autocorrelation property of white noise it has. However, the cross-correlation properties of m-sequences are not so ideal.

By shifting and adding a pair of sequences with the best cross-correlation coefficients selected from the m-sequences, the Gold-sequence is generated, which has the same number of bits as the m-sequence. Although the autocorrelation property of the Gold-sequence is inferior to that of the m-sequence, the cross-correlation coefficient between the generated Gold-sequences will not exceed the original m-sequence.

Walsh codes are derived from the Hadamard matrix. The greatest advantage of Walsh-sequence is that it has good cross-correlation and strong orthogonality. But the Walsh matrix is a square matrix, and the number of codes is equal to the number of bits of the sequence, which means that the number of Walsh-sequences is very limited.

Table 3: Parameters of our proposed modem.

Measurement parameter	Value
Communication band	35 kHz~45 kHz
Modulation scheme	FH–MFSK
Data rate	200/300 bit/s
Idle power consumption	24 mW
Receiving power consumption	0.6 W
Transmitting power consumption	6 W
Coding rate	1/2
Height	40 mm
Diameter	64 mm

The m-sequence is the longest period sequence that can be generated by n-level shift registers, and this sequence must be generated by nonlinear shift registers. It has many available frequency hopping patterns and has excellent autocorrelation and cross-correlation properties.

From the simulation results of Figure 5, it is not difficult to conclude that the other three sequences have better cross-correlation performance than the m-sequence, and they are not very different from each other. We choose the m-sequence which has a greater number of sequences and is more convenient to implement as our FH codes.

The main performance parameters for measuring FH codes are uniformity and randomness, both of which are well performed by m-sequences. FH codes can be determined by the parameters of m-sequence and the number of frequency hopping bands. The FH figure and period histogram used in this paper are shown in Figure 6.

As depicted in Figure 7, in the case of limited communication bandwidth, the larger the order of MFSK modulation is, the faster the information transmission rate will be, but there come the problems that the fewer frequency hopping bands, the greater mutual interference between code elements, and the higher BER is bound to be. When the error exceeds the correction capability of the error correcting code, information cannot be correctly restored. So, we have to make a trade-off between communication rate, modulation order, and the number of frequency hopping bands. Our system divides the communication band into 8 hopping bands, combined with the FFT frequency resolution of 97.66 Hz. M is set to 4 and 8 to adapt to different channel conditions and communication needs.

3.3. Software Workflow Description. Figure 8 illustrates the software flow of our acoustic modem. After the modem is powered up, the system is initialized, including kernel initialization, clock, UART (universal asynchronous receiver/transmitter), and ADC (analog-to-digital converter) initialization. The system works in a normal mode by default and can be switched to low power mode. Relevant parameters are set via the command line of UART. If the modem is in normal mode, the system will collect signal continuously. Starting from ADC interrupt, the receiving

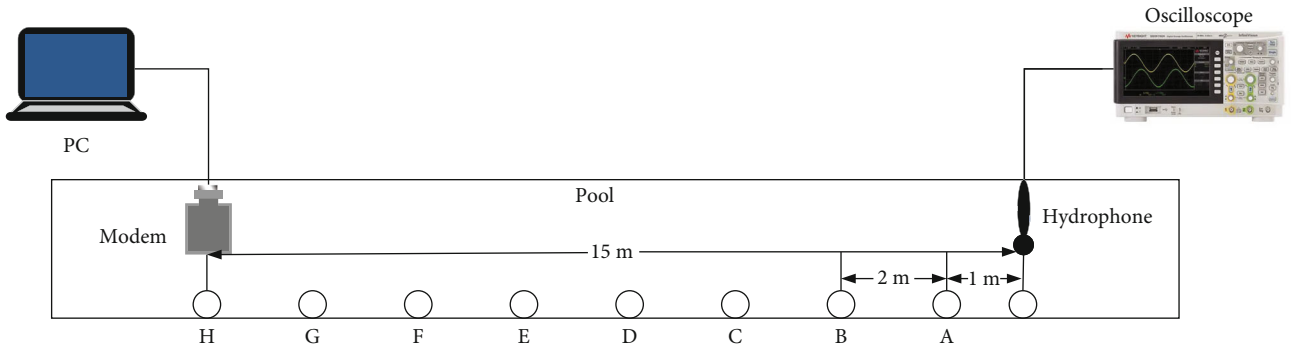

Figure 17: Schematic diagram of the experimental scene.

Table 4: Peak-to-peak values at different points.

Distance (m)	Peak-to-peak value (V)	Sound source level (dB)
1	0.3280	134.3
3	0.1390	136.4
5	0.0513	132.1
7	0.0860	139.6
9	0.0970	142.8
11	0.0840	143.3
13	0.0719	143.4
15	0.0600	143.0

algorithm will be executed to find the synchronization head and demodulate received signal; then results will be sent to the host. The UART interrupt indicates the receipt of a transmit command, and the system will execute the transmitting algorithm, modulate the signal, and transmit it out through the analog circuitry. If the system is in low power mode, it is normally in sleep state, and the modem will be periodically awakened by timer; then the related transmitting and receiving processes are performed as described above.

4. Hardware Board Design

In this section, we will introduce the hardware design of our acoustic modem. Figure 9 shows the hardware flow. The binary data input by user is interweaved by an interleaving matrix with a depth of 6, and then the channel convolutional code whose polynomial is (171,133) with a coding rate of 1/2 is utilized. After that, the digital signal modulated by the core processor is converted into a pulse width modulation (PWM) signal by digital-to-analog converter (DAC) with a maximum voltage of 3.3 V. After amplified by the power amplifier, the peak-to-peak value of 150 V is generated, and the signal is transmitted through the transceiver common circuit.

The STM32F767 has a low-power operation mode. In idle state, the system will enter the stop mod, where all external circuits such as AD/DA are turned off. Only the backup register, standby circuit, and RTC module maintain power supply. At this time, the overall operating current of our system is maintained below 0.2 mA, and the power consumption is about 2.4 mW (under 12 V).

In the passive reception mode, the preamble signal in this paper consists of three continuous single-frequency signals with different frequencies, which can be used as a wake-up signal to make the receiving system start the demodulation of coarse synchronization. It can also perform preliminary estimation of synchronization position at the same time, thereby reducing the computational complexity and power consumption of the system during synchronization, while improving the LFM synchronization performance and synchronization efficiency. Meanwhile, the overall working current is kept at 50 mA, and the power consumption is 600 mW (under 12 V).

When receiving, the acoustic signal is converted into the electrical signal by transducer, passed through a transceiver common circuit, filtered and amplified by preamplifier circuit and band-pass filter, and then amplified again by variable gain amplifier. Finally, the signal is sampled by the core processor's built-in 12-bit ADC and demodulated.

When the voice module is expanded, the user's voice instructions will be converted into text by the voice recognition module for subsequent operations. Texts demodulated at receiver are synthesized into speech by a speech synthesis circuit, so that the personnel at the receiving end can hear the command and take corresponding measures.

Next, we will introduce the hardware resources of our modem in detail.

4.1. Digital Signal Processor. As the core processor of a complex acoustic modem, the original data need to be encoded and modulated quickly to generate the transmitted signal when transmitting, and the underwater acoustic signals need to be identified, demodulated and restored in real time during reception. Therefore, the processor must meet the following conditions: since a large number of data processing and FFT/IFFT operations need to be carried out, the processor is required to have an excellent data processing capacity and can also support floating-point operations to speed up the operation speed and improve the execution efficiency of the system; as the core processor of a low-cost modem, on the premise of satisfying computing performance, the processor is required to have low cost and high reliability; at the same time, it also

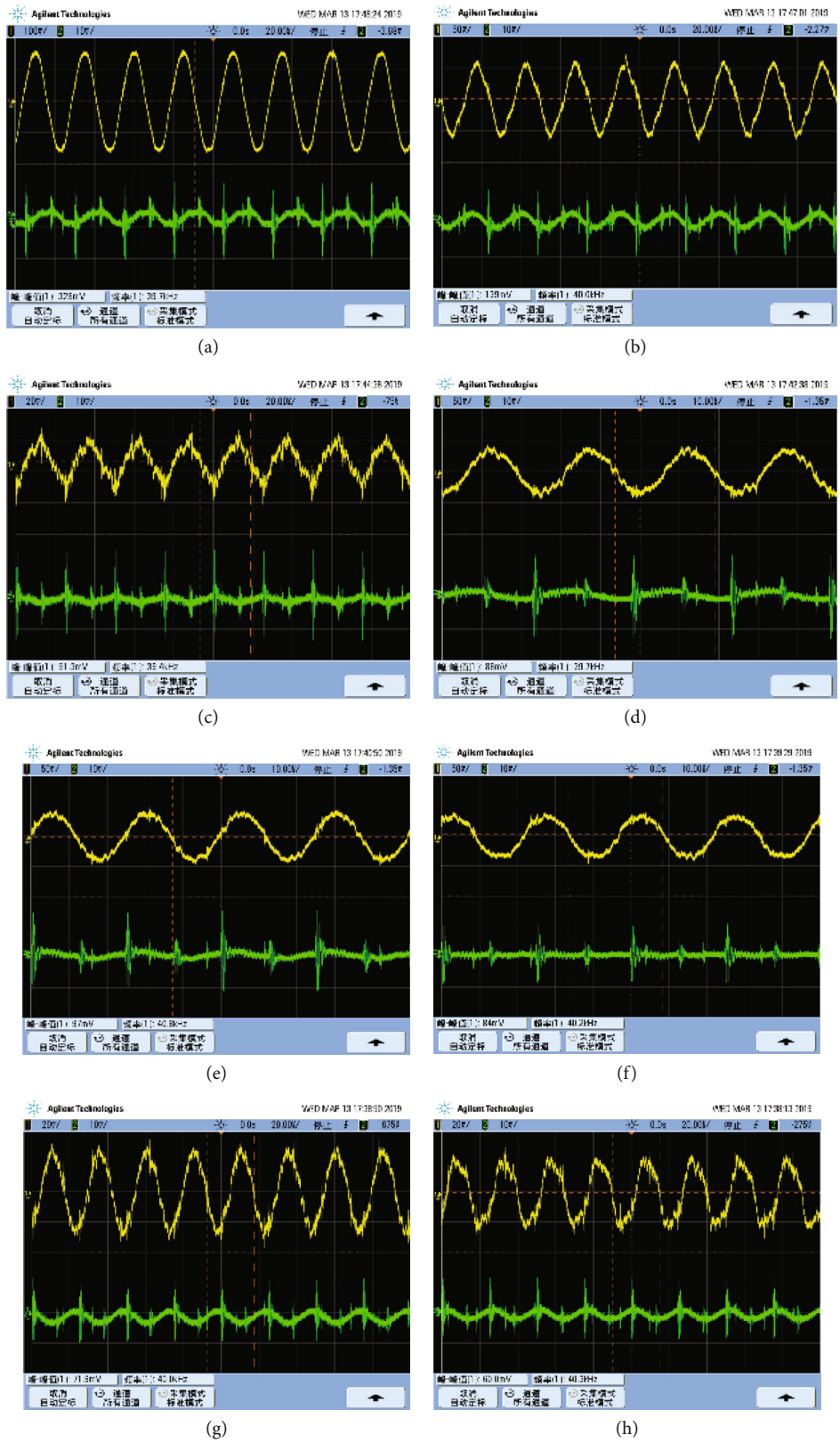

(a) (b) (c) (d) (e) (f) (g) (h)

Figure 18: Received waveforms in pool experiment.

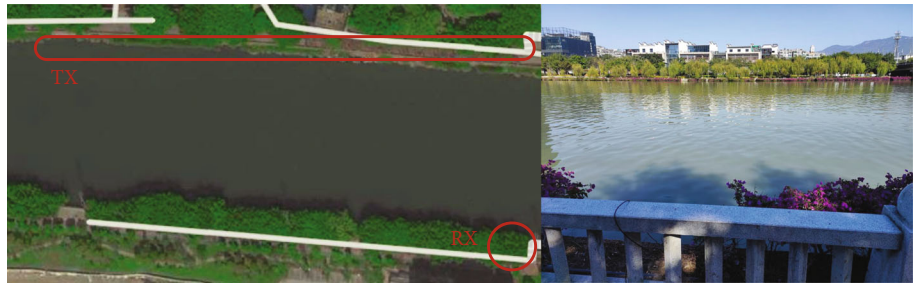

Figure 19: Field experiment at Guangming Port.

requires a small size for system integration and low power consumption to ensure the battery life.

According to above criterions, we take the STM32F7 chip based on Cortex-M7 as our core processor. Figure 10 shows its system architecture. The STM32F7 microcontroller can release the highest theoretical performance value of the Cortex-M7 core: at 216 MHz master frequency, the performance test can achieve 1082 CoreMark/462 DMIPS (Dhrystone Million Instructions executed Per Second). The Cortex-M7 core has a floating-point unit (FPU) that supports ARM double- and single-precision data processing instructions and data types; the high-speed embedded memory is integrated with up to 1 MB of flash and 512 KB of static random-access memory (SRAM). It also provides three 12-bit ADCs, two DACs, a low-power real time clock (RTC), and twelve universal 16-bit timers. Besides, it has standard and advanced communication interfaces, 2 universal direct memory access (DMA) controllers, and more other peripheral interfaces. With a budget price of $7, it is the ideal processor for our low-cost acoustic modem.

4.2. ADC and DAC. The underwater acoustic signals collected by the transducer are analog signals, which need to be converted into digital signals through ADC so that the subsequent signal processing can be performed. We use the STM32's built-in ADC acquisition module, which is a successive approximation analog-to-digital converter. It has up to 19 multiplexed channels, and the A/D conversion of these channels can operate in single-shot, continuous, sweep, or discontinuous sampling modes. The results of ADC are stored in a left or right justified 16-bit data register.

Since our acoustic modem needs to have the ability of real-time reception, the microcontroller unit (MCU) must perform calculations while receiving signals. Because it involves a lot of ADC data movement, if the MCU is directly responsible for this work, it will undoubtedly reduce the performance of the system, so we use DMA and double-buffering technology to solve this problem. DMA is used to provide high-speed data transfers between peripherals and memory or between memory and memory. Without any CPU operation, a direct data transfer path can be opened up between RAM and I/O devices through hardware, which can greatly improve the efficiency of CPU.

Because signals need to be received continuously, the double buffer design is adopted in this paper to prevent data loss. We open up two data buffer storage areas in the memory: buffer1 and buffer2. DMA controls the data collected by ADC and stores data in buffer1 and buffer2 in turn, and then the MCU kernel starts to process the acquired data.

Table 5: The parameters of the Guangming Port test channel.

Parameter	Value
Communication distance	100~300 (m)
Depth of transmitters	1 (m)
Depth of receiver	1 (m)
Depth of water	4 (m)
Number of test bits	10000

Table 6: BER over the test channel.

Distance (m)	BER (%)	
	FH–4FSK	FH–8FSK
100	0.02	0.17
150	0.15	0.4
200	0.08	0.25
250	0.03	0.11
300	0	0

4.3. Transmitting Module

4.3.1. Speech Recognition Chip. The speech recognition function is mainly completed by LD3320. This chip is a speech recognition chip based on nonspecific human speech recognition technology, which means the voice sent by any individual can be correctly recognized without recording training. The chip can set up to 50 keywords in advance, and these keywords can be freely modified according to different application scenarios. The only limitation is the length of each keyword, while the short communication commands for divers are almost less than 30 words, which meets our design requirements. Its main working method is to recognize the input voice in the preedited list of key words and send the instructions of the recognized keywords to MCU.

4.3.2. Power Amplifier. Linear power amplifier has low working efficiency, complex circuit structure, and large volume, which is not conducive to integration. Therefore, we use

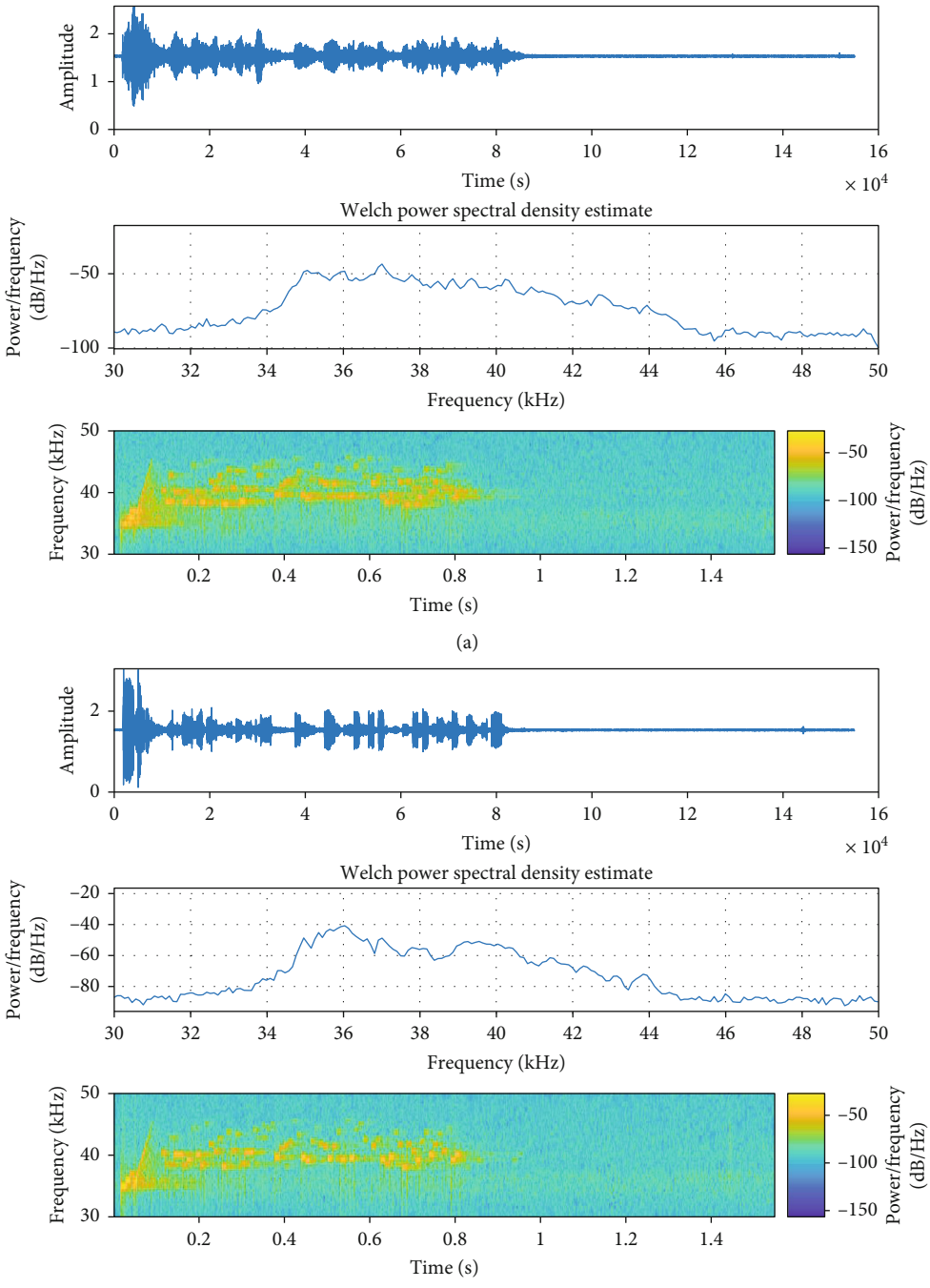

Figure 20: Continued.

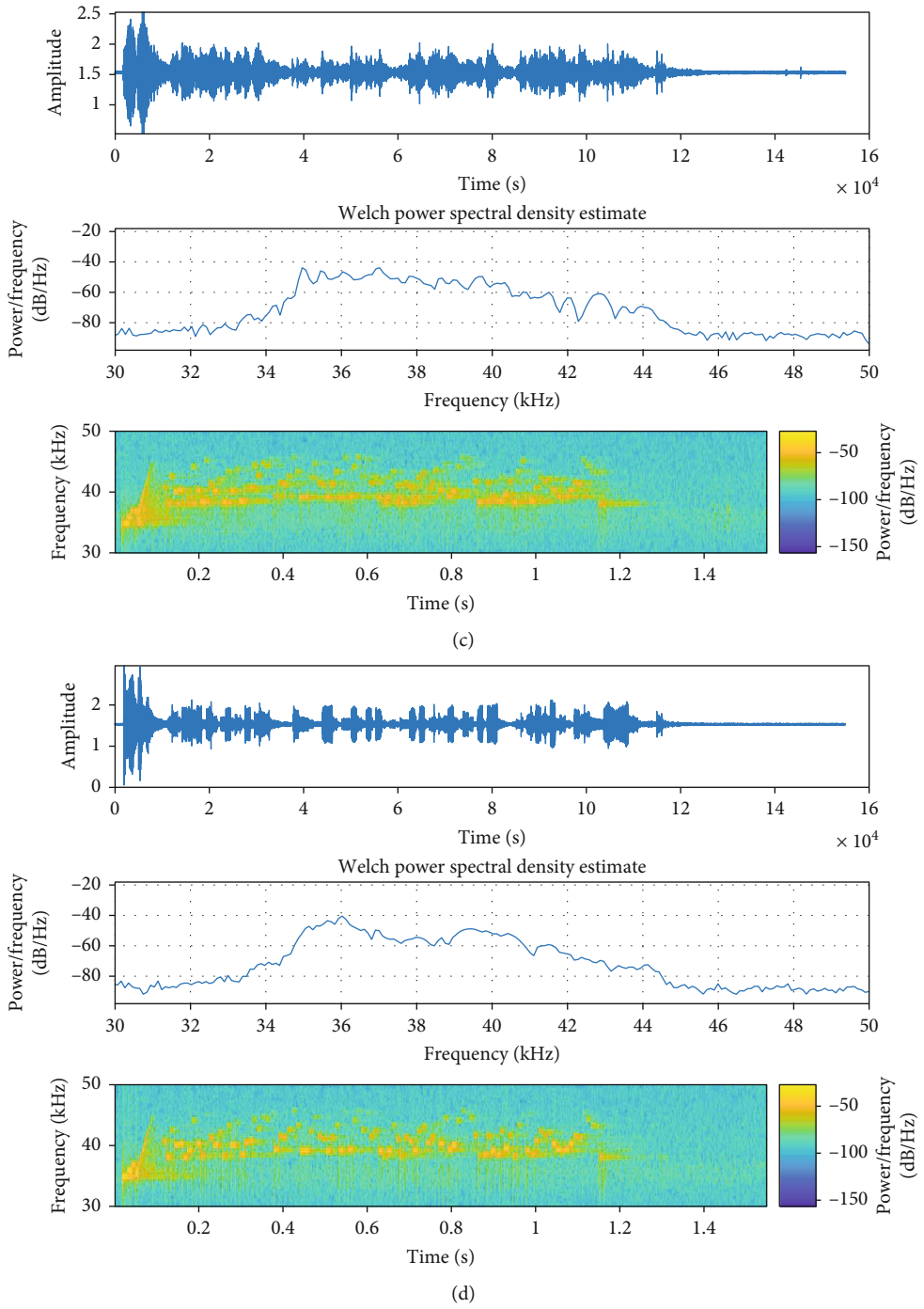

Figure 20: Received signals at (a, c) 150 m and (b, d) 300 m. (a) Received FH–8FSK signal, 150 m. (b) Received FH–8FSK signal, 300 m. (c) Received FH–4FSK signal, 150 m. (d) Received FH–4FSK signal, 300 m.

the class D MOS (metal oxide semiconductor) tube as power amplifier tube. Our modem adopts IRLU3410 as the switch tube of the power amplification circuit. In addition, the integrated chip MCP1415/16 is used to design the driving circuit as the input stage of MOS tube power amplifier to improve the current driving ability. MCP1415/16 is a high-speed MOSFET driver produced by an American microchip company. It has a high output current, low impedance, and short propagation delay. The PWM signal from MCU first enters the driving circuit to provide a large current for the MOS tube, then enters the gate of the MOS tube for signal amplification, and is finally transmitted through the transceiver common circuit.

4.3.3. Transceiver Common Circuit. Our acoustic modem uses a half-duplex communication mode, so the output of power amplifier and the input of preamplifier are connected to the same transducer. In the transmitting state, the transmitting power amplifier circuit will generate a large voltage about 150 V. Loading such a large signal to

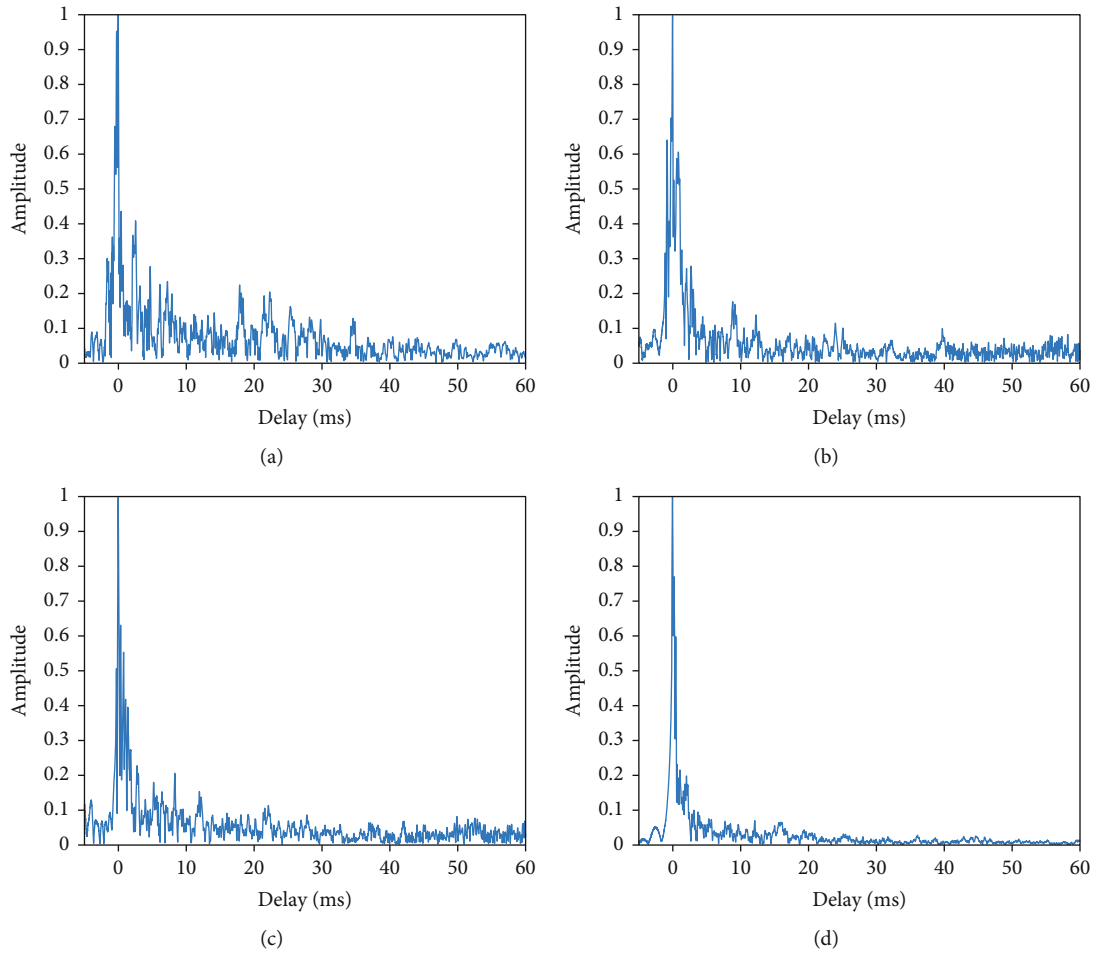

Figure 21: Impulse response functions at different distances. (a) Channel impulse response, 150 m. (b) Channel impulse response, 200 m. (c) Channel impulse response, 250 m. (d) Channel impulse response, 300 m.

Table 7: The parameters of Wuyuan Bay test channel.

Parameter	Value
Communication distance	500 (m)
Depth of transmitters	0.5~2 (m)
Depth of receiver	0.5~2 (m)
Depth of water	8 (m)
Number of test bits	50000

the preamplifier will absolutely damage the receiver circuit, so we designed a transceiver common circuit.

The transceiver common circuit is formed by reverse parallel connection of power resistor R1 and a group of diodes D2 and D3. When our modem is ready to transmit signal, the diode D2 is on, and the conduction voltage of D2 is 0.7 V. At the same time, the excess energy is radiated through R1. Another diode D4 keeps the preamplifier circuit in low voltage and protects the receiving circuit.

4.4. Receiving Module

4.4.1. Preamplifier. Since the underwater acoustic signal received by transducer is extremely weak and contains a large amount of environmental noise, it needs to be amplified and filtered to meet the subsequent processing requirements of MCU. Our system uses the AD8421 chip to realize the preamplification of the received signal. With a hundred times gain, the chip still has an input bandwidth of 1 MHz, which basically covers all the frequency bands occupied by UAC. Its amplification characteristic is also quite excellent, the settling time required for 10 times amplified output is as short as 0.6 μs, which is suitable for fast time-varying underwater channels.

4.4.2. Band-Pass Filter. In order to cooperate with the front-end's flexible and interchangeable transducer, our system adds a programmable band-pass filter to realize the selection and switching of different bandwidths. This filter is realized by the MAX7491 chip of the MAXIM Company. MAX7491 is a dual-channel frequency-selectable capacitor filter. We only need to provide the chip with clocks of different frequencies to control the center frequency of the filter. The center frequency can be selected range from 0 to 40 kHz. Through the design of the peripheral circuit, MAX7491 can be controlled to work in different modes such as low-pass, high-pass, and band-pass. The power

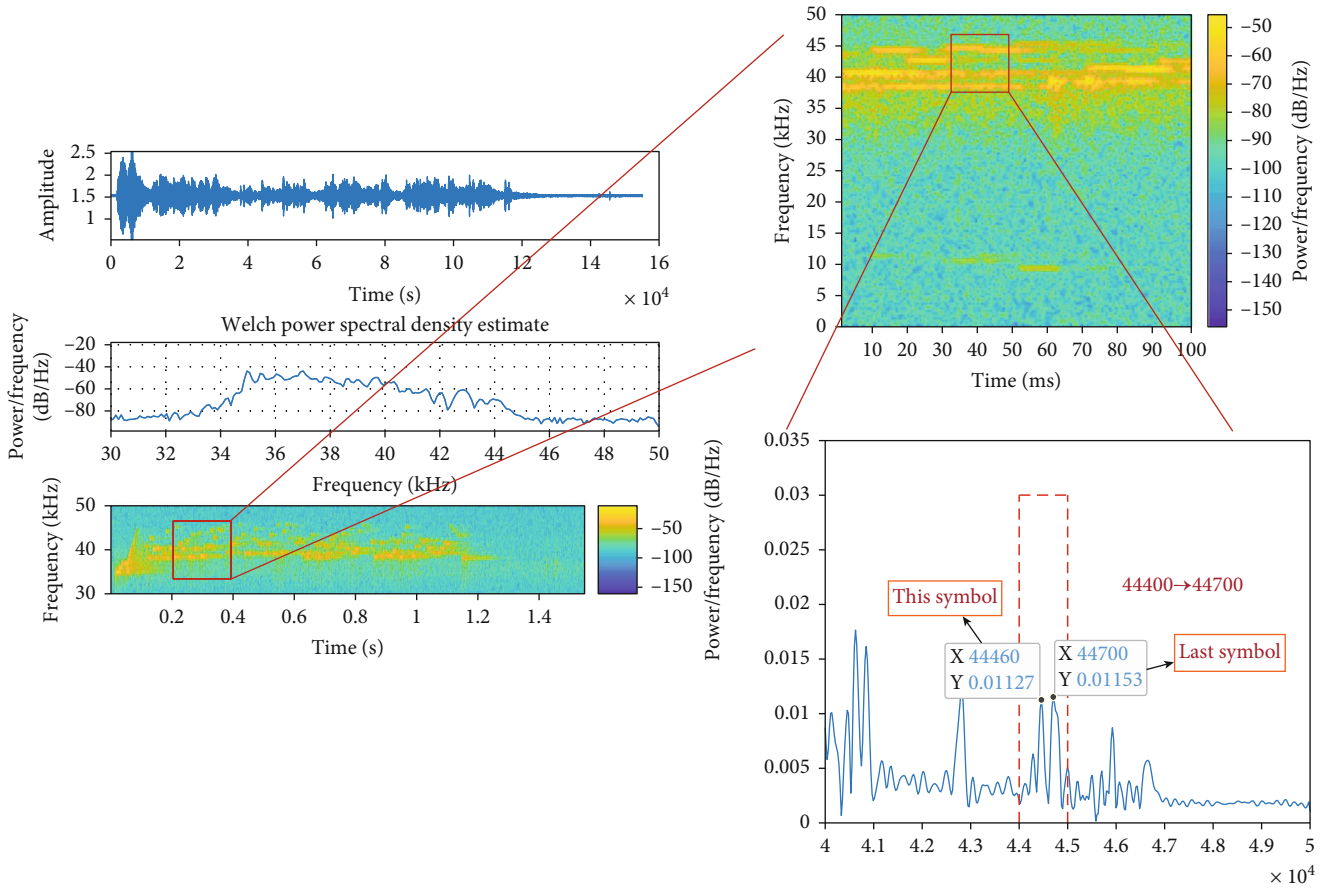

Figure 22: Error demodulation under FH scheme due to multipath effect.

Figure 23: Field experiment at Wuyuan Bay.

consumption of the chip is also relatively low, which is more in line with the requirements of our system.

The band-pass filter we designed allows to pass the frequency range of 33.17 kHz to 46.43 kHz. Its gain reaches a maximum of 53 dB at the center frequency of 38.9 kHz, and the signals in other frequencies are obviously suppressed. The amplitude-frequency characteristic of our band-pass filter is shown in Figure 11.

4.4.3. Programmable Voltage Amplifier. Considering the realization of automatic gain control (AGC) of input signal, it is necessary to process the variable gain amplification before the signal is sent to AD. Our modem uses the AD8338 as the programmable amplifier chip. The dynamic gain of AD8338 ranges from 0 to 80 dB, and different gain control can be achieved by inputting different analog voltage values to the 7th pin of the chip. The power consumption of AD8338 is also relatively controllable. When the gain is 40 dB, the operating current of the circuit is only 3 mA, and the additional power consumption brought to the system is only 10 mW.

4.4.4. Speech Synthesis Chip. The function of speech synthesis is mainly realized by SYN6288. The chip supports texts in a variety of formats, and the synthesized voice is clear, natural, accurate, and highly recognizable. With intelligent analysis and processing functions, it can correctly handle identify phone numbers, dates, and common metrics. The chip's package is small and supports the sleep function with low power consumption. Its main working method is to synthesize the corresponding voice after receiving the instructions sent by MCU and play them out.

4.5. Prototype of Our Modem. The hardware design of our underwater acoustic modem is shown in Figure 12, which is cylindrical in shape with a diameter of 6.5 cm and a height of 1.5 cm. The digital and analog boards are separated to facilitate the design and avoid mutual interference.

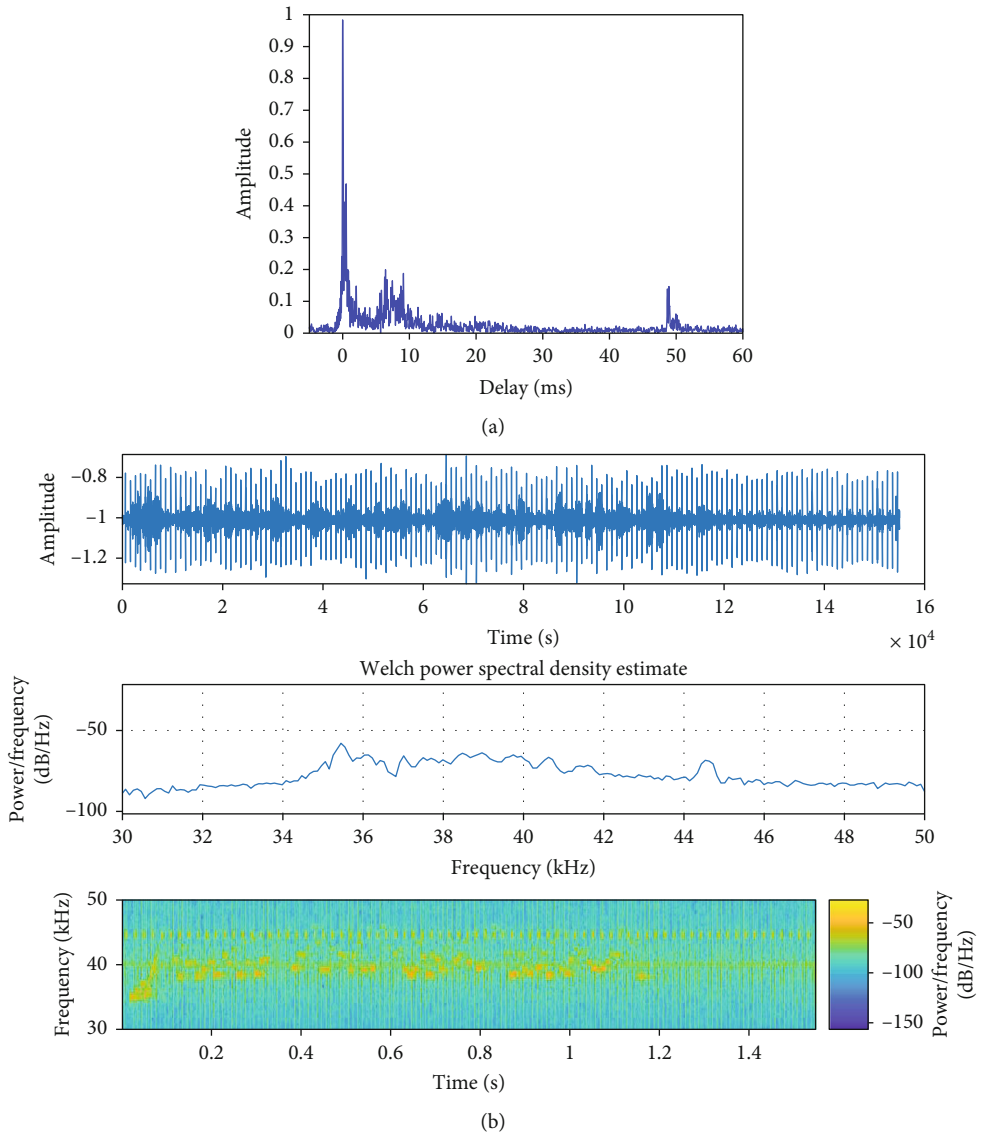

Figure 24: (a) Impulse response function and (b) received signal in Wuyuan Bay (500 meters).

Traditional transducers use cylindrical or spherical ceramics, which are relatively bulky and have solidified parameters that cannot be customized for diverse communication needs. A sheet ceramic customized in this paper is shown in Figure 13. The emission angle is adjusted through the structural design to ensure that the transducer can not only meet the need of sensitivity but also significantly reduce the cost and the volume of integrated package.

Under the premise of customization and miniaturization of the piezoelectric transducer, the circuit module and the transducer are packaged in an integrated manner. Figure 14 gives the finished product and schematic diagram of the package design. The parameters of our implemented modem are summarized in Table 3.

5. Experimental Results

In this section, we first simulate the communication scheme on the computer and then design several experiments under different experimental scenarios to fully verify the performance of our acoustic modem.

5.1. Computer Simulation. The test was performed with 10000 bits under multipath channel, which is generated by the Bellhop model as shown in Figure 15. Parameters of Bellhop were set to a communication distance of 1000 m and the transducer depth of 5 m.

Figure 16 indicates the simulation results. The addition of convolutional coding may theoretically perform worse at low SNR due to more severe interference; however, it can significantly reduce the BER of the communication when SNR is higher than -5 dB. Compared with the FH–8FSK scheme, FH–4FSK can effectively improve the reliability of the system by spacing out the modulation frequencies at the expense of a portion of the rate.

5.2. Sound Source Level Test. In order to test the sound source level of our developed acoustic modem, experiments

have been conducted in an anechoic pool. The pool is about 25 meters long and 5 meters wide, the shallowest is 1.2 meters, and the deepest is 1.9 meters. Our modem is used as the transmitting source, and the standard hydrophone is used as the receiver and connected to an oscilloscope. Figure 17 illustrates the experimental location, and a total of 9 nodes are set. The rightmost node is the first node, and the distance between farthest nodes is 15 meters. Every two nodes are spaced 2 meters apart except the first one. During this experiment, the modem sends signals with a frequency of 40 kHz sequentially starting from the second node, and received waveforms are recorded with the oscilloscope as shown in Figure 18.

According to the definition of sound source level mentioned above, the sound source level can be calculated from the peak-to-peak value of waveforms at each position. As shown in Table 4, the source level of our acoustic modems ranges from 132.1 dB to 143.4 dB.

5.3. Outfield Experiment

5.3.1. Test in a River. In December 2021, our acoustic modem was tested in Guangming Port for communication experiment. Guangming Port is an inland river in the urban area of Fuzhou, with a width of 50~140 m. The scene is schematically shown in Figure 19.

We fixed the receiver on one side of the shore without moving and set the transmitter on the other side to do communication tests at different distances, testing 10,000 bits for two schemes at each point. The maximum test distance was 300 m due to the limitation of space. Parameters of this experiment are listed in Table 5. Other parameters of modem can be seen in Table 3.

The waveforms, power spectrums, and time-frequency diagrams of received signals at these two positions are also given in Figure 20. It can be seen that the SNR of the received signal is about 15 dB. The frequencies from 35 to 45 kHz are useful signals, while the out-of-band noise is attenuated by 20 dB. Each frequency point in the time-frequency diagram is clearly visible, while the multipath effect can also be distinguished, which is manifested as a certain delay for each frequency point on the time axis. The BER results are tabulated in Table 6, it shows that the BER of our modem are in the order of 10^{-3}, and the FH–4FSK does show better stability, which are consistent with the simulation results.

Generally, as the communication distance increases, the attenuation of acoustic energy will also increase, and the SNR at the receiver is consequently reduced, which leads to a higher BER of reception. However, the amplifier circuit of our modem can keep the SNR of received signal in a good condition at the distance of 300 m. From the simulation in Figure 16, the BER is maintained at a relatively smooth lower limit when the SNR is above a certain threshold, at which time the multipath effect has a greater influence on the communication accuracy. Figure 21 shows the multipath channels at different distances.

It can be seen that, probably due to the distribution of underwater obstacles, received signals in a closer distance are more severely affected by multipath channel due to more reflected path arrivals superimposed. We calculated their average time delay extensions, and the results are 14.89 ms, 11.97 ms, 10.39 ms, and 7.64 ms from near to far, which contributes more to the BER than the reduction of SNR. So, the experimental results of Guangming Port will occur. If the communication distance is further extended, the SNR may become worse, which will lead to the higher BER. And we will look for a more suitable site for testing in the future.

After analysis, the main cause of bit errors is that under the frequency hopping scheme, there may be multiple consecutive frames of signals in the same hopping band, and the previous frame of signal is extended to the subsequent frames by multipath effect, thus affecting the demodulation, which also matches the performance of the experimental results. For example, as shown in Figure 22, the original FFT demodulation result of the signal in this frame should be 44400 Hz, but due to the residual delay of last symbol in the same hopping band, the demodulation result is wrongly turned into 44700 Hz. This is a problem inherent in the FH communication system itself, which can be improved by optimizing the frequency hopping sequence in the subsequent development of modem. Another interesting phenomenon is that most of the erroneous demodulation is concentrated in a similar higher frequency part. This is probably due to the fact that the design of our transducer is not flat enough in the communication band, resulting in less energy in the higher frequencies, which is also a point that can be improved subsequently.

5.3.2. Test in Wuyuan Bay. We conducted another experiment in the Wuyuan Bay of Xiamen City to test the performance of our micromodem in a more complex environment immediately and chose FH–4FSK as the test scheme. The structure of the experimental scenario is shown in Figure 23. Due to the fluctuation of the tide, the depth of the communication modem varies with time. The experimental parameters are listed in Table 7 below.

Figure 24 shows the measured Wuyuan Bay's channel and information of received signal. The detected channel is more complicated than that of Guangming Port, and there has noise generated by the navigation of ships. It is also subjected to unknown interference of 45 kHz in the communication frequency band. The received SNR is about 7 dB, and the BER results of data transmission obtained by the final statistics are 0.3%, which proves that our acoustic modem has a good performance.

6. Conclusions

In this paper, we design and implement an acoustic modem based on STM32F767. It has the advantages of miniaturization, low cost, and low power consumption and is suitable for a variety of underwater IoT scenarios. A frame structure for underwater communication is proposed for signal synchronization, and a convolutional code–block interleaving–-frequency hopping–MFSK scheme is analyzed to overcome underwater interference and achieve stable underwater acoustic communication. The size of modem is decreased

by hardware design and integrated package. Finally, the reliability of our modem was verified through several indoor and outdoor field tests.

Data Availability

The data used to support the findings of this study come from indoor and outdoor experiments. They are counted within the article and available from the corresponding author.

Conflicts of Interest

The authors declare that they have no conflicts of interest.

Authors' Contributions

Hongbin Chen and Yi Zhu contributed equally to this work.

Acknowledgments

The authors would like to thank the National Natural Science Foundation of China (62071401, 62001404) and Xiamen Ocean and Fishery Development Special Fund Project (21CZB 015HJ10).

References

[1] D. B. Kilfoyle and A. B. Baggeroer, "The state of the art in underwater acoustic telemetry," *IEEE Journal of Oceanic Engineering*, vol. 25, no. 1, pp. 4–27, 2000.

[2] I. F. Akyildiz, D. Pompili, and T. Melodia, "Underwater acoustic sensor networks: research challenges," *Ad Hoc Networks*, vol. 3, no. 3, pp. 257–279, 2005.

[3] Tritech, "Micron Modem-Acoustic Modem," https://www.tritech.co.uk/product/micron-data-modem.

[4] Sonardyne, "Modem 6 acoustic modems," https://www.sonardyne.com/products/underwater-acoustic-modems/.

[5] "Teledyne Benthos," http://www.teledynemarine.com/Acoustic_Modems?BrandID=2.

[6] LinkQuest Inc, "Underwater acoustic modem models," http://link-quest.com/html/models1.htm.

[7] DSPComm, "Aquacomm: underwater acoustic modems," https://dspcommgen2.com/aquacomm-underwater-wireless-modem/.

[8] EvoLogics, "Underwater acoustic modems," https://evologics.de/acoustic-modems.

[9] W. Bin Abbas, N. Ahmed, C. Usama, and A. A. Syed, "Design and evaluation of a low-cost, DIY-inspired, underwater platform to promote experimental research in UWSN," *Ad Hoc Networks*, vol. 34, pp. 239–251, 2015.

[10] J. A. Neasham, G. Goodfellow, and R. Sharphouse, "Development of the Seatrac miniature acoustic modem and USBL positioning units for subsea robotics and diver applications," in *OCEANS 2015-Genova*, pp. 1–8, Genova, Italy, May 2015.

[11] X. Li, M. Zhu, and Y. Wu, "Low-power system design for underwater acoustic modems," in *Proceedings of the 10th International Conference on Underwater Networks & Systems*, pp. 1-2, Arlington VA USA, October 2015.

[12] S. Misra, A. Mukherjee, D. Pal, and S. Dalal, "U-OCEAN: an underwater omnidirectional communication environment using acoustic sensor nodes," in *2017 IEEE International Conference on Advanced Networks and Telecommunications Systems (ANTS)*, pp. 1–6, Bhubaneswar, India, December 2017.

[13] W. Lee, J. H. Jeon, and S. J. Park, "Micro-modem for short-range underwater communication systems," in *2014 Oceans-St. John's*, pp. 1–4, St. John's, NL, Canada, September 2014.

[14] W. A. van Kleunen, N. A. Moseley, P. J. Havinga, and N. Meratnia, "Proteus II: design and evaluation of an integrated power-efficient underwater sensor node," *International Journal of Distributed Sensor Networks*, vol. 11, no. 10, 2015.

[15] B. C. Renner, J. Heitmann, and F. Steinmetz, "Ahoi: inexpensive, low-power communication and localization for underwater sensor networks and μAUVs," *ACM Transactions on Sensor Networks (TOSN)*, vol. 16, no. 2, pp. 1–46, 2020.

[16] Y. Su, L. Dong, Z. Zhou, X. Liu, and X. Wei, "A general embedded underwater acoustic communication system based on advance STM32," *IEEE Embedded Systems Letters*, vol. 13, no. 3, pp. 90–93, 2021.

[17] F. B. Jensen, W. A. Kuperman, M. B. Porter, H. Schmidt, and A. Tolstoy, *Computational Ocean Acoustics*, vol. 794, Springer, New York, 2011.